

ISOLATED STAR FORMATION: A COMPACT HII REGION IN THE VIRGO CLUSTER¹

ORTWIN GERHARD¹, MAGDA ARNABOLDI^{2,3},
 KENNETH C. FREEMAN⁴, SADANORI OKAMURA⁵

¹Astronomisches Institut, Universität Basel, Venusstrasse 7, CH-4102 Binningen, Switzerland

²I.N.A.F., Osservatorio Astronomico di Capodimonte, 80131 Naples, Italy

³I.N.A.F., Osservatorio Astronomico di Pino Torinese, 10025 Pino Torinese, Italy

⁴R.S.A.A., Mt. Stromlo Observatory, 2611 ACT, Australia

⁵Department of Astronomy, School of Science, University of Tokyo, Tokyo, 113-0033, Japan
Astrophysical Journal Letters, in press (scheduled Dec. 1, 2002)

ABSTRACT

We report on the discovery of an isolated, compact HII region in the Virgo cluster. The object is located in the diffuse outer halo of NGC 4388, or could possibly be in intracluster space. Star formation can thus take place far outside the main star forming regions of galaxies. This object is powered by a small starburst with an estimated mass of $\sim 400 M_{\odot}$ and age of ~ 3 Myr. From a total sample of 17 HII region candidates, the present rate of isolated star formation estimated in our Virgo field is small, $\sim 10^{-6} M_{\odot} \text{arcmin}^{-2} \text{yr}^{-1}$. However, this mode of star formation might have been more important at higher redshifts and be responsible for a fraction of the observed intracluster stars and total cluster metal production. This object is relevant also for distance determinations with the planetary nebula luminosity function from emission line surveys, for high-velocity clouds and the in situ origin of B stars in the Galactic halo, and for local enrichment of the intracluster gas by Type II supernovae.

Subject headings: stars: formation – HII regions – galaxies: ISM – galaxies: star clusters – galaxies: abundances – intergalactic medium

1. INTRODUCTION

Stars are usually observed to form in galaxies, that is, in disks, dwarfs, and starbursts. In radio galaxies, star formation may be triggered by energetic jet outflows (e.g., Bicknell et al. 2000). The HII region we describe here shows that isolated star formation takes place in the diffuse outskirts of galaxies, at the boundary of, if not already in, Virgo intracluster space.

In nearby galaxy clusters, a diffuse intracluster star component has been inferred from surface brightness measurements (Bernstein et al. 1995) and detection of individual stars (e.g., Arnaboldi et al. 1996, Ferguson et al. 1998, Feldmeier 2002). Its origin may be explained readily by dynamical processes acting on low-surface brightness disks and dwarfs, which unbind the stars from these galaxies (Moore et al. 1999). However, gas may be efficiently removed from infalling galaxies by ram pressure stripping (Quilis et al. 2000, Gavazzi et al. 2001), or may be tidally dissolved, or could fall into the cluster as pristine clouds. Some of this gas may form stars, which would also contribute to the diffuse component. We discuss here the current rate of such star formation from isolated compact HII regions (ICHIIs) and from jet induced star formation in a Virgo cluster field.

2. AN HII REGION IN VIRGO: OBSERVED PROPERTIES

The target object was found in an emission line survey for planetary nebulae in a Virgo intracluster field, centred at $\alpha(J2000)12 : 25 : 31.9$, $\delta(J2000)12 : 43 : 47.7$, using H α and [OIII] narrow band and V+R broad band filter

photometry (Arnaboldi et al. 2002, Okamura et al. 2002), with Suprime-Cam on the Subaru Telescope. Because of the large H α to [OIII] flux ratio the (unresolved) object was classified as a candidate compact HII region.

A spectrum was taken at UT4 of the VLT at Paranal, on the night of April 14, 2002, with FORS2 in MOS mode. The observations were carried out with GRISM-150I and the order separation filter GG435+81, giving a wavelength coverage of 4500–10200 Å and a dispersion of 6.7 Å pix⁻¹. The slit width was 1.4 arcsec, and the angular scale along the slitlet was 0.126 arcsec pix⁻¹. The total exposure time was 7×1800 s. The nights were clear but not photometric; the mean seeing was better than 1.0 arcsec. Spectrophotometric standard stars were observed at the beginning and end of the night, but cirrus clouds at these times made the flux calibration uncertain.

The data reduction was carried out using standard tasks in IRAF, using an arc lamp wavelength calibration and observations of a spectrophotometric standard star. The spectrum was corrected for atmospheric extinction, using a table for La Silla².

The wavelength and flux-calibrated spectrum is shown in Figure 1: it clearly shows a blue continuum and a number of emission lines at Virgo redshift: H α , H β , H γ , [OIII] λ 5007 and λ 4959, [SII] λ 6717 + 6731, and [SIII] λ 9069. We do not resolve H α and [NII] λ 6548, and the [SII] λ 6717, 6731 lines, respectively, and we do not see the weaker [OI] λ 6300, [OIII] λ 4363, and [SIII] λ 6312 lines. The H γ line lies close to the blue end of the spectrum, and the [SIII] λ 9069 line in a region of strong sky emission.

¹Based on observations carried out at UT4 of the VLT, Paranal, Chile, which is operated by the European Southern Observatory.

²No correction for atmospheric refraction is needed since FORS2 has an atmospheric dispersion corrector.

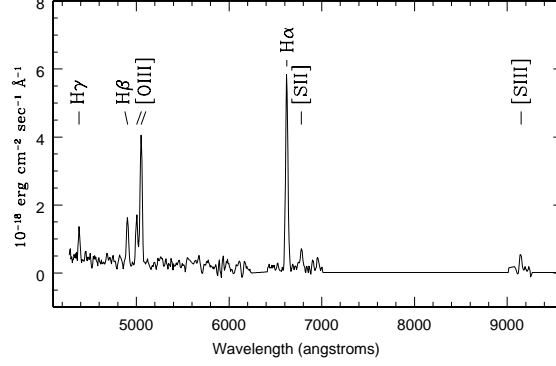


FIG. 1.— Observed emission spectrum.

TABLE 1
OBSERVED AND REDDENING-CORRECTED EMISSION LINE FLUXES RELATIVE TO $H\beta$.

Line	λ Å	observed flux rel. to $H\beta$	de-reddened flux rel. to $H\beta$
$H\gamma$	4340	0.58	0.71
$H\beta$	4861	1.00	1.00
[OIII]	4959	1.03	0.99
[OIII]	5007	3.05	2.91
[NI]	5200	0.08	
$H\alpha$	6563	4.30	2.89
[NII]	6583	0.75	0.50
[SII]	6717+6731	0.40	0.26
[SIII]	9069	0.30	0.14

[NI] identification uncertain.

[NII] λ 6583 flux from two-Gaussian fit.

$H\alpha$ flux is corrected for corresponding [NII] λ 6548 emission.

The observed emission lines and their uncorrected and reddening-corrected fluxes normalized to $H\beta$ are listed in Table 1. The errors in the fluxes are approximately 10% of the $H\beta$ flux, and larger at the blue edge of the spectral range. The $H\alpha$ and $[NII]\lambda 6548$ lines are unresolved, with the $[NII]\lambda 6583$ line appearing in the red wing of $H\alpha$. From a two-Gaussian fit to the combined emission we estimate the line ratio $[NII]\lambda 6583/(H\alpha + [NII]\lambda 6548) \simeq 0.17$. This is consistent with the value expected for an HII region with the large observed $[OIII]\lambda 5007/H\beta$ ratio; see below. The $H\alpha$ flux given in the table is that measured as the total flux in the line reduced by one third that in $[NII]\lambda 6583$. The observed Balmer decrement $H\alpha/H\beta$ then becomes 4.3.

If the intrinsic Balmer decrement has the theoretical value of 2.89 for large optical depth (case B) and temperature $T = 10^4$ K, then $E(B-V) = 0.40$ and $A_V = 1.23$ mag. Most of this reddening is intrinsic to the source, as the galactic absorption to nearby galaxies in the Virgo cluster is about $A_V \simeq 0.12$. Line fluxes were corrected for reddening using this value of $E(B-V)$ and the reddening curve of Cardelli et al. (1989). Compared to $H\beta$, the corrected $H\gamma$ flux is about 1.5 times larger than expected; however, we cannot regard the $H\gamma$ flux as reliable, because the line lies right at the edge of the spectrum where uncertainties in the grism response, sky subtraction and determination of the continuum level will be at their worst.

The corrected line ratios $[OIII]\lambda 5007/H\beta = 2.91$, $[NII]\lambda 6583/H\alpha = 0.17$, and $[SII]\lambda\lambda 6717, 6731/H\alpha = 0.09$ place the object clearly into the domain of HII regions in Figs. 1,2 of Veilleux & Osterbrock (1987; VO87). This is also confirmed by the weakness (non-detection) of $[OI]\lambda 6300$ in the spectrum.

Because the flux calibration using our standard stars is uncertain, we transformed it to the Jacoby (1989) m_{OIII} calibration of the imaging photometry from Suprime-Cam (Arnaboldi et al. 2002). This gives a total $m_{OIII} = 25.7$ magnitude for this object. Because of the $[OIII]$ filter width used in the emission line survey, this flux includes both the $[OIII]\lambda\lambda 4959, 5007$ lines, as well as the flux from the continuum. Using the spectrum to measure the fraction of light in the continuum, we can correct to the magnitude in the $\lambda 5007$ line only: $m_{5007} = 26.15$. From the standard star-calibrated spectrum, we would get $m_{5007} = -2.5 \log F_{5007} - 13.74 = 25.1$. The difference gives us a factor 2.63, by which to rescale F_{5007} to match the photometric calibration. The rescaled total flux in the $[OIII]\lambda 5007$ Å line is $F_{5007} = 11.0 \times 10^{-17} \text{ erg s}^{-1} \text{ cm}^{-2}$. With $E(B-V) = 0.4$ the dereddened flux becomes $F_{5007} = 4.0 \times 10^{-16} \text{ erg s}^{-1} \text{ cm}^{-2}$. The fluxes in the other emission lines can then be inferred from the dereddened line ratios in Table 1; in particular the $H\alpha$ flux becomes $3.9 \times 10^{-16} \text{ erg s}^{-1} \text{ cm}^{-2}$.

The measured V-band continuum flux from the spectrum, when applying the same calibration and correcting for reddening, becomes $F_V = 7.0 \times 10^{-16} \text{ erg s}^{-1} \text{ cm}^{-2}$. The corresponding dereddened apparent magnitude is $m_V = 24.2$. Absolute magnitudes and fluxes will be computed for a nominal Virgo distance modulus of 31.16, corresponding to 17 Mpc distance (Tonry et al. 2001). However, we will sometimes keep the distance dependence by writing $D = d_{17} \text{ Mpc}$. The continuum $m_V = 24.2$ then gives $M_V = -7.0$.

3. PHYSICAL PARAMETERS

Metallicity: The high values of $[OIII]/H\alpha = 1.0$ and $[OIII]/H\beta = 2.9$ indicate subsolar metallicity. The VO87 diagrams are not ideal for estimating metallicities, as discussed by Dopita et al. (2000), but from Figs. 2,3 of that paper we estimate $Z \simeq 0.4$ and an ionization parameter $q \simeq 4 \times 10^7$ ($\log U = -2.9$). Both very low and high metallicities are not consistent with their model results and these line ratios. A more accurate determination is in principle possible using the S_{23} parameter, defined as $S_{23} = ([SII]\lambda\lambda 6717, 6731 + [SIII]\lambda\lambda 9069, 9532) / H\beta = 0.75$, where we have used the theoretical ratio $[SIII]\lambda 9532/[SIII]\lambda 9069 = 2.48$. From the empirical calibration of Díaz & Pérez-Montero (2000) we then find $12 + \log(O/H) \simeq 8.08 \pm 0.2$ (about 0.15 to 0.25 solar with or without the depletion factor used by Dopita et al. 2000). In our case, S_{23} has additional uncertainties due to the weak $[SII]$ line and the bright NIR sky lines, which might affect the $[SIII]$ flux. In the following, we therefore adopt $Z \simeq 0.4$.

Temperature, density, ionization parameter: Unfortunately, the S/N of the spectrum is not large enough to detect the weak $[OIII]\lambda 4363$ and $[NII]\lambda 5755$ lines used to determine electron temperature, nor do we have lines to determine the electron density. In the following we use $T_e = 10^4$ K when needed.

Estimates of the ionization parameter from the Sulfur lines, using equations (8) and (6) of Díaz et al. (2000) give similar values to that from the VO87 diagrams: $[SII]\lambda\lambda 6717, 6731/[SIII]\lambda\lambda 9069, 9532 \simeq 0.53$ gives $\log U = -2.5$, and $[SII]\lambda\lambda 6717, 6731/H\beta \simeq 0.26$ and metallicity 0.4 solar gives $\log U = -2.9$.

Luminosities: From above, the total V-band luminosity is

$$L_V = 4\pi D^2 F_V = 2.4 \times 10^{37} d_{17}^2 \text{ erg s}^{-1}. \quad (1)$$

The $H\alpha$ flux is

$$L_{H\alpha} = 4\pi D^2 F_{H\alpha} = 1.3 \times 10^{37} d_{17}^2 \text{ erg s}^{-1}. \quad (2)$$

The total number of H-ionizing photons (Osterbrock 1989) with recombination coefficients α_B and $\alpha_{H\alpha}^{\text{eff}}$ for $T = 10^4$ K is

$$Q(H^0) = 2.96 L_{H\alpha} / h\nu_{H\alpha} = 1.3 \times 10^{49} d_{17}^2 \text{ s}^{-1}. \quad (3)$$

Stellar mass and age of starburst: The ratio $Q(H^0)/L_V$ decreases rapidly with the mass of the most massive surviving O stars, i.e., the age of the starburst. Using the Starburst99 model of Leitherer et al. (1999) for metallicity 0.4 solar and normal Salpeter IMF, we determine an age of 3.3 Myr. Once this is known, the Lyman continuum luminosity can be used to infer the total mass in the corresponding starburst; we obtain $400 M_\odot$. The number of O stars involved is 1–2, so these numbers must be considered as averages.

Mass and size of gas cloud: We can estimate the total mass of ionized hydrogen from (Osterbrock 1989)

$$M_{HII} = Q(H^0) m_p / [n_e \alpha_B] = 420 n_{100}^{-1} d_{17}^2 M_\odot, \quad (4)$$

where $n_{100} = n_e / 100 \text{ cm}^{-3}$ and m_p denote the electron density and proton mass. Around early O stars, the H Strömgren radius is

$$r_{HII} = \left[\frac{M_{HII}(1+y^+)}{(4\pi/3)n_e m_p} \right]^{1/3} \simeq 3.5 n_{100}^{-2/3} d_{17}^{2/3} \text{ pc}, \quad (5)$$

where $y^+ \simeq 0.1$ is the fraction by number of ionized helium. This is indeed much smaller than the photometric spatial resolution (about $0''.7 = 57d_{17} \text{ pc}$). The column density is

$$N_{\text{HII}} = M_{\text{HII}}/(\pi r_{\text{HII}}^2) = 1.3 \times 10^{21} n_{100}^{1/3} d_{17}^{2/3} \text{ cm}^{-2}. \quad (6)$$

From the inferred extinction and metallicity we may estimate the intervening hydrogen column density from the local interstellar medium relation (Bohlin, Savage & Drake 1978), using

$$N(\text{H}) \simeq 5.9 \times 10^{21} \text{ cm}^{-2} \text{ mag}^{-1} E_{B-V} Z_{\odot}/Z \sim 6 \times 10^{21} \text{ cm}^{-2}. \quad (7)$$

If the neutral hydrogen is in a much denser shell than the HII, then we can use the HII radius also to estimate its total mass

$$M_{\text{H}} = \pi r_{\text{HII}}^2 \times 2N(\text{H})m_p = 3600 M_{\odot}. \quad (8)$$

The star formation efficiency would then be around 10%.

4. DISCUSSION

The compact HII-region is located about 3.4 (17 kpc projected distance) north and 0.9 (4.4 kpc) west of NGC 4388, almost perpendicular to the disk plane of this galaxy and 45° away from the nearest part of the very extended emission-line region (VEELR) discussed by Yoshida et al. (2002). The radial velocity inferred from the emission lines is 2670 km s^{-1} , whereas the galaxy has $v_r = 2520 \text{ km s}^{-1}$. The near-coincidence of these numbers may indicate that the HII region is, or once was, part of the NGC 4388 system. From the large radial velocity relative to the Virgo center ($v_r \sim 1.8\sigma_{\text{Virgo}}$) and from the Tully-Fisher distance of NGC 4388 (Yasuda et al. 1997), both are probably falling through the cluster core.

This HII region is powered by a small stellar association or star cluster, with an estimated mass of $\sim 400 M_{\odot}$ and age of $\sim 3 \text{ Myr}$ for a normal IMF. If it is a young cluster, it must have a radius smaller than that of the HII region ($\sim 3.5 \text{ pc}$). Clusters with these parameters have short relaxation times and dissolve by internal dynamical processes; within a few 10^8 yr the stars would be added to the diffuse stellar population nearby.

The formation of such objects is thus possible far outside the main star forming regions in galaxies. Perhaps the most plausible explanation for the observed position and velocity of the HII region relative to NGC 4388 is that it is already unbound and moving on a different orbit in the cluster potential. In this case we would be seeing intracluster star formation. If on the other hand its true distance from NGC 4388 is comparable to the projected distance so that it is still bound, we would have discovered a small star-forming knot in the far outer halo of NGC 4388 far from any other star formation activity. This would have a velocity in the frame of the galaxy comparable to the circular velocity ($\simeq 200 \text{ km s}^{-1}$) of NGC 4388. In fact, in the Subaru field that contained our ICHII region, Arnaboldi et al. (2002) found a small sample of similar candidate objects, among which 7 candidates are located in the outskirts of M86, at a distance of 10–15 kpc in a disturbed region which probably also contains diffuse $\text{H}\alpha$ emission, and 1 such object in the outer parts of M84.

What has triggered the recent onset of star formation in this remote cloud? Notice that with its radial velocity, it

will have moved $\sim 4 \text{ kpc}$ relative to the Virgo cluster, and $\sim 500 \text{ pc}$ relative to NGC 4388, in the lifetime of the massive stars. Thus these stars will essentially have formed in situ. A possible model could be that the cloud was compressed after entering the hot intracluster medium (ICM). While the typical pressure of the ICM ($n_e T \sim 10^4 \text{ K/cm}^3$) is far smaller than the internal pressure inferred from typical HII region parameters ($n_e \sim 100/\text{cm}^3$; $T \sim 10^4 \text{ K}$), it could be comparable to that of the surrounding neutral or molecular cloud traced by the absorption. The ionized region may be reexpanding into the surrounding cloud and into the ICM – the mass of the cluster is not large enough to bind the HII region.

Reanalysing the Subaru field photometry, we have also detected a number of extended emitters in both [OIII] and $\text{H}\alpha$, with colors similar to the confirmed compact HII region. These are peaks in more extended emissions, and lie at distances 11–33 kpc along the direction of the VEELR identified by Yoshida et al. (2002) towards the NE of NGC 4388. These objects have relatively low excitation ([OIII]/ $\text{H}\alpha \simeq 0.6$, in agreement with Fig. 6 of Yoshida et al. 2002), and show continuum emission near the limiting magnitude of the combined (V+R) image (Arnaboldi et al. 2002). Their half-light radii are similar in the combined continuum and in the [OIII] and $\text{H}\alpha$ images, which further supports the notion that these distant sources have underlying continuum emission, and are thus ionized by OB stars rather than by the nucleus of NGC 4388. From the discussion of Yoshida et al. (2002) it is likely that this star formation is induced by the jet or ionization cone.

Yoshida et al. (2002) proposed that the VEELR observed to the NE of NGC 4388 could be the debris of a past interaction. Although our ICHII region is 2.6 arcmin away from the nearest part of the VEELR, it could also be associated with such tidal debris. The gas in this ICHII region seems unlikely to come from ram pressure stripping of the gas in NGC 4388, because the peculiar velocity of the ICHII region relative to the systemic velocity of the Virgo cluster is even larger than for NGC 4388 itself. (We thank B. Moore for this comment.)

The total intracluster star formation rate (ISFR) estimated from the candidates in this field is small, however. Counting the 8 ICHII candidates near M86 and M84 plus 3 intracluster candidates, including that studied here, and the 6 best extended candidates, gives a total of 17 star-forming HII regions in the Subaru field. If the density of these objects is typical for the Virgo cluster core, these would correspond to $\sim 10^3$ such objects throughout Virgo. If we adopt similar parameters to those inferred for the HII region here (conservatively), we obtain from these candidates a total ISFR of ~ 10 times $\sim 400 M_{\odot}$ per 3 Myr, in a surveyed area of 918 arcmin^2 , i.e., $\sim 10^{-6} M_{\odot} \text{ arcmin}^{-2} \text{ yr}^{-1}$. For comparison, the intracluster luminosity inferred from planetary nebulae in the Subaru field is $\sim 10^7 L_{B,\odot} \text{ arcmin}^{-2}$. However, it appears not impossible that at higher redshifts, when the environment of infalling galaxies was more gas-rich, formation of stars directly from this intracluster gas could have been an important part of the origin of intracluster stars in Virgo.

The existence of compact HII regions in Virgo, beyond its intrinsic interest, is relevant for a few other issues as well. Firstly, the massive stars ionizing the gas explode as

type II supernovae and enrich the Virgo ICM with metals. This process adds to the main metal content of the ICM, which is believed to have occurred at high redshift when most of the stars in the cluster ellipticals and bulges formed (Renzini 1999). From the ISFR inferred above, the present expected supernova rate is $\sim 10^{-8} \text{ arcmin}^{-2} \text{ yr}^{-1}$. SN II from isolated star formation could provide the enrichment inferred for the Ly α clouds in Virgo (Tripp et al. 2002). Because our ICHII region contains only 1-2 O stars, observations of the enrichment from such objects in isolated regions might give constraints on the element yields of individual supernovae. Newly formed stars from this material could then have a range of abundance ratios similar to old Galactic halo stars (Argast et al. 2000).

Secondly, compact HII regions may affect distance determinations with the planetary nebula luminosity function (PNLF, Jacoby et al. 1992). The [OIII] luminosity of this ICHII region places it at the bright end of the luminosity function inferred from [OIII] emission line surveys. In a sufficiently deep offband control image its continuum light would be visible, leading to removal from the PN sample. However, this does require a deep image, and moreover

there are a few HII candidates in the Subaru field for which the continuum is not detected. A few unrecognized such objects per galaxy or intracluster field could cause the distance to these fields to be underestimated. It is unclear whether this may account for the lower average distance inferred by the PNLF compared to surface brightness fluctuations (Ciardullo et al. 2002).

Thirdly, if compact ICHII regions exist in galaxies generally, they could be the birth places of distant B stars in the Galactic halo, some of which are too far from the disk to have been ejected from there into the halo (Conlon et al. 1992). Most likely, their birth places would be distant high velocity clouds. At this time, however, there is no evidence for star formation in galactic high-velocity clouds.

We thank R. Scarpa for efficient help at UT4, J. Alcalá for independently checking line fluxes, and A. Capetti for a helpful discussion. OG thanks the Swiss Nationalfonds for support under grant 20-64856.01. This research has made use of the NASA extragalactic database.

REFERENCES

- Argast, D., Samland, M., Gerhard, O.E., & Thielemann, F.-K. 2000, *A&A*, 356, 873
 Arnaboldi, M., et al. 1996, *ApJ*, 472, 145
 Arnaboldi, M., et al. 2002, *AJ*, in press
 Bernstein, G.M., et al. 1995, *AJ*, 110, 1507
 Bicknell, G.V., et al. 2000, *ApJ*, 540, 678
 Bohlin, R.C., Savage, B.D., & Drake, J.F. 1978, *ApJ*, 224, 132
 Cardelli, J.A., Clayton, G.C., & Mathis, J.S. 1989, *ApJ*, 345, 245
 Ciardullo, R., et al. 2002, *ApJ*, 577, 31
 Conlon, E.S., Dufton, P.L., Keenan, F.P., McCausland, R.J.H., & Holmgren, D. 1992, *ApJ*, 400, 273
 Díaz, A.I., Pérez-Montero, E. 2000, *MNRAS*, 312, 130
 Díaz, A.I., Castellanos, M., Terlevich, E., & García-Vargas, M.L. 2000, *MNRAS*, 318, 462
 Dopita, M.A., Kewley, L.J., Heisler, C.A., & Sutherland, R.S. 2000, *ApJ*, 542, 224
 Feldmeier, J.J. 2002, *IAU Symp.* 209, Intracluster Planetary Nebulae, ASP, in press, astro-ph/0201452
 Ferguson, H., Tanvir, N.R., & von Hippel, T. 1998, *Nature*, 391, 461
 Gavazzi, G., et al. 2001, *ApJ*, 563, L23
 Jacoby, G.H. 1989, *ApJ*, 339, 39
 Jacoby, G.H., et al. 1992, *PASP*, 104, 599
 Leitherer, C., et al. 1999, *ApJS*, 123, 3
 Moore, B., Lake, G., Quinn, T., & Stadel, J. 1999, *MNRAS*, 304, 465
 Okamura, S., et al. 2002, *PASJ*, in press
 Osterbrock, D.E. 1989, *Astrophysics of Gaseous Nebulae and Active Galactic Nuclei*, University Science Books, Mill Valley
 Quilis, V., Moore, B., & Bower, R. 2000, *Science*, 288, 1617
 Renzini, A. 1999, in *Chemical Evolution from Zero to High Redshift*, eds. J. Walsh, M. Rosa (Berlin, Springer), 185
 Tonry, J.L. et al. 2001, *ApJ*, 546, 681
 Tripp, T.M., et al. 2002, *ApJ*, 575, 697
 Veilleux, S., & Osterbrock, D.E. 1987, *ApJS*, 63, 295 (VO87)
 Yasuda, N., Fukugita, M., Okamura, S. 1997, *ApJS*, 108, 417
 Yoshida, M., et al. 2002, *ApJ*, 567, 118